SHAPLEYPIPE: HIERARCHICAL SHAPLEY SEARCH FOR DATA PREPARATION PIPELINE CONSTRUCTION

Jing Chang

SICS, Shenzhen University 2350273007@email.szu.edu.cn

Shuyuan Zheng[⊠]

Osaka University zheng@ist.osaka-u.ac.jp

Chang Liu

SICS, Shenzhen University 2300271084@email.szu.edu.cn

Rui Mao[⊠]

SICS, Shenzhen University mao@szu.edu.cn

Jinbin Huang

SICS, Shenzhen University jbhuang@szu.edu.cn

Jianbin Qin[⊠]

SICS, Shenzhen University qinjianbin@szu.edu.cn

November 3, 2025

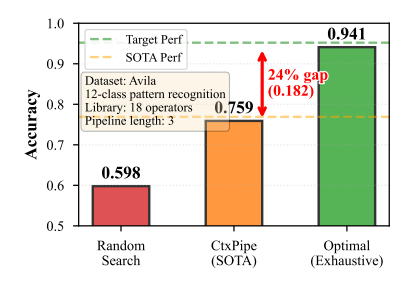
ABSTRACT

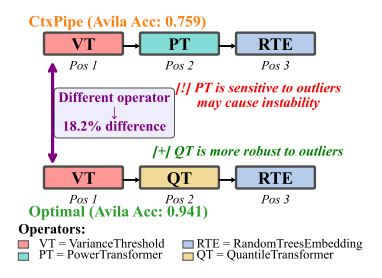
Automated data preparation pipeline construction is critical for machine learning success, yet existing methods suffer from two fundamental limitations: they treat pipeline construction as black-box optimization without quantifying individual operator contributions, and they struggle with the combinatorial explosion of the search space (N^M configurations for N operators and pipeline length M). We introduce ShapleyPipe, a principled framework that leverages game-theoretic Shapley values to systematically quantify each operator's marginal contribution while maintaining full interpretability. Our key innovation is a hierarchical decomposition that separates category-level structure search from operator-level refinement, reducing the search complexity from exponential to polynomial. To make Shapley computation tractable, we develop: (1) a Multi-Armed Bandit mechanism for intelligent category evaluation with provable convergence guarantees, and (2) Permutation Shapley values to correctly capture position-dependent operator interactions. Extensive evaluation on 18 diverse datasets demonstrates that ShapleyPipe achieves 98.1% of high-budget baseline performance while using 24% fewer evaluations, and outperforms the state-of-the-art reinforcement learning method by 3.6%. Beyond performance gains, ShapleyPipe provides interpretable operator valuations (ρ =0.933 correlation with empirical performance) that enable data-driven pipeline analysis and systematic operator library refinement.

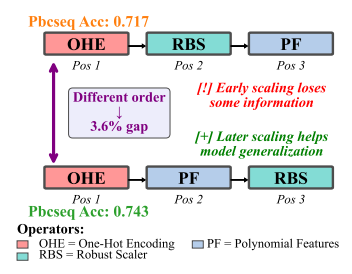
1 Introduction

Data preparation remains the most time-consuming phase in machine learning workflows, typically consuming 70-80% of project time [1,2]. The construction of effective data preparation pipelines, sequences of operations such as missing value imputation, feature scaling, and feature selection, critically determines downstream model performance [3]. However, this construction process relies heavily on manual expertise and trial-and-error, making it a prime target for automation. While Automated Machine Learning (AutoML) has made significant progress in automating algorithm selection and hyperparameter tuning [4,5]. The automated construction of data preparation pipelines faces a fundamental challenge: combinatorial explosion. Given N available operators and M pipeline positions, the search space contains N^M possible configurations. For instance, with 25 operators and a pipeline length of 6, practitioners face over 244 million candidates. Exhaustive evaluation is clearly infeasible.

Existing automated pipeline construction methods fall into three main categories, each with critical limitations: Search-based methods (grid search [6], random search [7], Bayesian optimization [8,9]) struggle with high-dimensional discrete space and require thousands of evaluations. Evolutionary algorithms (TPOT [5], SAGA [10]) are prone to premature convergence and lack theoretical guarantees [11]. Reinforcement learning approaches (CtxPipe [12], HAI-AI [13]) represent the current state-of-the-art, formulating pipeline construction as a sequential decision problem [14]. Despite sophisticated







- (a) Performance Gap on Avila
- (b) Operator Selection Comparison
- (c) Pipeline Structure Comparison

Figure 1: Motivating examples showing operator selection and ordering both matter. (a) On Avila dataset, CtxPipe (0.759) vs. optimal (0.941) shows 24% gap. (b) Operator choice matters: Using PowerTransformer (PT, sensitive to outliers) vs. QuantileTransformer (QT, robust to outliers) at position 2 yields 18.2% difference. (c) On Pbcseq dataset, ordering matters: identical operators {One-Hot Encoding (OHE), Polynomial Features (PF), Robust Scaler (RBS)} achieve 0.743 vs 0.717 accuracy (3.6% gap).

neural architectures and contextual information, these methods exhibit substantial performance gaps and require extensive offline training, as we demonstrate next.

Motivating Example. To illustrate the fundamental challenge in automated pipeline construction, we designed a controlled experiment on the Avila dataset. We constructed a search space with 18 operators and pipeline length 3, yielding $18^3=5,832$ possible configurations, small enough for complete exhaustive evaluation but large enough to be meaningful. Pipeline performance is measured by training a LogisticRegression classifier on the pipeline-transformed data and evaluating its prediction accuracy on a validation set.

We reproduced CtxPipe [12] within this search space and compared it against exhaustive search. As shown in Figure 1a, CtxPipe achieves 0.759 accuracy, while exhaustive search reveals the true optimal pipeline achieving 0.941 accuracy. There is a substantial 24% performance gap between them. This experiment demonstrates that existing methods fail to discover high-quality pipelines even when the optimal solution exists within their search space. Analyzing the two pipelines (Figure 1b), we observe that they differ primarily in operator selection: CtxPipe selects PowerTransformer at position 2, which is sensitive to outliers and may cause instability, while the optimal pipeline uses the more robust QuantileTransformer. This may suggest that operator selection impacts performance, but is this always the dominant factor?

To validate this hypothesis on an even smaller and more controllable scale, we designed a second experiment on the Pbcseq dataset (Table 1), exhaustively evaluating all $5^3=125$ pipelines from 5 selected operators. Figure 1c reveals a different insight: two pipelines using the *exact same three operators*: OneHotEncoder, PolynomialFeatures, RobustScaler, but in different orderings, achieve 0.743 vs 0.717 accuracy (3.6% gap). The suboptimal ordering applies RobustScaler before PolynomialFeatures, the optimal delays scaling until after engineering. This experiment demonstrates that operator ordering can be as critical as operator selection.

The above experiments reveal two key insights: (1) state-of-the-art methods leave substantial performance on the table, and (2) both operator selection and position-dependent ordering matter. In summary, existing solutions mainly suffer from two core limitations: (1) Lack of systematic operator evaluation method to consider inherent functionality and the position of the operator simultaneously in a pipeline; (2) High computational complexity in analyzing the dependency between operators. Therefore, a principled framework that can quantify each operator's marginal contribution while accounting for complex, position-dependent interactions is a pressing need.

Game theory offers an ideal model to the comprehensive evaluation framework design. We observe that pipeline construction naturally maps to a cooperative game: operators are players, model accuracy is the collective payoff, and we seek to attribute this payoff fairly to individual contributors. The Shapley value, a solution concept from cooperative game theory, satisfies this requirement by computing each player's average marginal contribution across all possible coalitions. However, three fundamental challenges stand between this elegant theory and practical implementation. Exact Shapley computation requires exponential evaluations, making naive application infeasible. Classical Shapley values assume order-independence, yet pipeline operators exhibit strong position-dependent effects. Finally, treating all operators uniformly ignores their natural grouping into functional categories (e.g., scaling, engineering), leading to redundant search.

In this paper, we introduce ShapleyPipe, a novel framework that addresses these challenges through three key technical innovations. To address the first limitation, we first formulate pipeline construction as a cooperative game where operators are players and pipeline performance is the collective payoff. This enables us to quantify each operator's marginal contribution using position-specific Shapley values. For the second limitation, to overcome the exponential complexity of computing Shapley values, we develop a hierarchical decomposition strategy. Specifically, we exploit the natural categorical structure of

operator libraries to factorize the search into two tractable stages: category-level structure search followed by within-category operator refinement. Finally, we address the challenge of efficiently evaluating abstract categories through a Multi-Armed Bandit (MAB) mechanism that intelligently selects representative operators for category assessment, providing provable regret bounds while minimizing pipeline evaluations. In summary, our main contributions can be listed as follow:

- We are the first to formalize data preparation pipeline construction as a cooperative game and introduce positionspecific Shapley values to quantify each operator's marginal contribution while capturing order-dependent interactions.
- We propose a Hierarchical search framework ShapleyPipe, decomposing the exponential search space into categorylevel structure search and operator-level refinement, reducing the search complexity from exponential to polynomial with theoretical approximation guarantees.
- We propose a Multi-Armed Bandit mechanism, which is an efficient category evaluation approach with provable convergence guarantees, avoiding exhaustive enumeration while ensuring high-quality representative selection.
- On 18 benchmark datasets, ShapleyPipe achieves 98.1% of high-budget baseline performance using 24% fewer evaluations, outperforms state-of-the-art RL by 3.6%, and produces interpretable operator valuations.

2 PROBLEM FORMULATION

In this section, we formally define the components of a data preparation pipeline and formulate the pipeline construction task as a constrained optimization problem. We conclude by highlighting the fundamental challenge of credit assignment, which motivates our novel game-theoretic approach.

2.1 Preliminaries: Operators and Pipelines

Definition 1 (Data Preparation Operator). A data preparation operator is a deterministic function $o: \mathcal{D} \to \mathcal{D}'$ that transforms a dataset \mathcal{D} into a modified dataset \mathcal{D}' [15]. Let $\mathcal{O} = \{o_1, o_2, \dots, o_N\}$ denote the library of all available operators.

Definition 2 (Data Preparation Pipeline). A pipeline of length M is an ordered sequence $P = [p_1, p_2, \ldots, p_M]$, where each $p_j \in \mathcal{O} \cup \{\emptyset\}$. The null operator \emptyset represents "no operation," allowing for effective pipeline lengths less than M. Pipeline execution applies operators sequentially:

$$Pipeline(P, \mathcal{D}) = p_M \circ p_{M-1} \circ \dots \circ p_1(\mathcal{D}) \tag{1}$$

The full pipeline search space, $\Pi(\mathcal{O}, M) = (\mathcal{O} \cup \{\emptyset\})^M$, has a cardinality of $(N+1)^M$, which grows exponentially with M

Definition 3 (Performance Function). Given a dataset $\mathcal{D} = \{(x_i, y_i)\}_{i=1}^n$, a base learner \mathcal{A} , and an evaluation protocol \mathcal{E} (e.g., k-fold cross-validation), the performance function $v : \Pi(\mathcal{O}, M) \to [0, 1]$ maps any pipeline P to a performance score:

$$v(P) = \mathcal{E}(\mathcal{A}(Pipeline(P, \mathcal{D}_{train})), \mathcal{D}_{val})$$
(2)

Each evaluation of v(P) is computationally expensive, as it involves fitting the pipeline, transforming data, training the learner, and validating its performance.

2.2 The Pipeline Construction Problem

With the preliminary definitions established, we can now state the automated pipeline construction problem. The primary objective is to find the pipeline that yields the maximum possible performance for a given dataset, learner, and operator library.

Problem Statement. Given a dataset \mathcal{D} , an operator library \mathcal{O} , and a base learner \mathcal{A} , the goal is to find an optimal pipeline P^* that maximizes the performance function v:

$$P^* = \arg \max_{P \in \Pi(\mathcal{O}, M)} v(P) \tag{3}$$

While the ultimate goal is to find P^* , the prohibitively large search space $\Pi(\mathcal{O}, M)$ makes exhaustive evaluation impossible. Thus, the practical challenge lies in designing a search strategy that is computationally efficient. An ideal method should not only converge to a high-quality solution but should do so with a minimal number of expensive pipeline evaluations.

3 A Game-Theoretic Framework FOR PIPELINE CONSTRUCTION

To address the challenge of quantifying operator contributions, we reformulate pipeline construction as a cooperative game. This allows us to leverage the Shapley value to provide a principled solution for operator attribution.

3.1 Principled Operator Valuation via Shapley Values

3.1.1 Cooperative Games and the Shapley Value

Cooperative game theory provides a mathematical foundation for fairly allocating a collective payoff among a set of collaborating players [16].

Definition 4 (Cooperative Game). A cooperative game is formally defined as a pair (\mathcal{N}, v) , where:

- $\mathcal{N} = \{1, 2, \dots, n\}$ is a finite set of players.
- $v: 2^{\mathcal{N}} \to \mathbb{R}$ is the characteristic function, which maps each subset of players (a coalition) $S \subseteq \mathcal{N}$ to its value, or payoff, v(S). By convention, the value of the empty coalition is zero, $v(\emptyset) = 0$.

The central question in cooperative game theory is how to distribute the total payoff $v(\mathcal{N})$ among the players in a way that is "fair" and reflects their individual contributions. The Shapley value [12] stands out as a unique solution that satisfies several desirable fairness axioms, such as efficiency, symmetry, and linearity [17].

Definition 5 (Shapley Value). The Shapley value $\phi_i(v)$ of a player $i \in \mathcal{N}$ in a game (\mathcal{N}, v) is its weighted average marginal contribution over all possible coalitions it could join:

$$\phi_i(v) = \sum_{S \subset \mathcal{N} \setminus \{i\}} \frac{|S|!(n-|S|-1)!}{n!} [v(S \cup \{i\}) - v(S)] \tag{4}$$

The term $[v(S \cup \{i\}) - v(S)]$ represents the marginal contribution of player i to the coalition S. The weighting factor ensures that every possible ordering in which players could form the grand coalition \mathcal{N} is equally likely.

Example 1 (3-Player Game) Consider 3 players $\{A,B,C\}$ with a characteristic function defined as: $v(\{A\}) = v(\{B\}) = v(\{C\}) = 0$; $v(\{A,B\}) = 50$, $v(\{A,C\}) = 30$, $v(\{B,C\}) = 40$; and $v(\{A,B,C\}) = 80$. Player A's marginal contributions depend on the context:

- Joining the empty coalition: $v(\lbrace A \rbrace) v(\emptyset) = 0$.
- Joining after B: $v(\{A, B\}) v(\{B\}) = 50$.
- Joining after C: $v({A, C}) v({C}) = 30$.
- Joining after B and C: $v(\{A, B, C\}) v(\{B, C\}) = 40$.

Averaging these contributions over all 3! = 6 possible player orderings with the appropriate weights yields the Shapley values: $\phi_A = 26.67, \phi_B = 28.33, \text{ and } \phi_C = 25. \text{ Note that they sum to the total payoff: } 26.67 + 28.33 + 25 = 80 = v(\{A, B, C\}).$

3.1.2 Mapping Pipeline Construction to a Cooperative Game

The problem of data preparation pipeline construction can be naturally mapped to the cooperative game framework, providing a principled way to quantify operator contributions. The mapping is as follows:

- Players \mathcal{N} : The set of all available data preparation operators, $\mathcal{O} = \{o_1, \dots, o_N\}$. Each operator is a "player" that can contribute to the final model's performance.
- Coalition S: A subset of operators, $S \subseteq \mathcal{O}$. This represents a toolkit of available operators for building a pipeline.
- Characteristic function v(S): The performance of the best possible pipeline that can be constructed using only the operators in the coalition S. This value represents the maximum achievable payoff for that group of players.
- Goal: Compute the Shapley value ϕ_i for each operator o_i . This value quantifies the operator's average marginal contribution to pipeline performance, enabling principled operator valuation.

This game-theoretic formulation is powerful because it moves beyond evaluating fixed pipelines. Instead, it assesses the intrinsic value of each operator by considering its potential contribution in a vast array of contexts (i.e., in combination with

all possible subsets of other operators). The resulting Shapley value for an operator o_i provides a clear, interpretable answer to the question: "On average, how much performance improvement does including operator o_i bring to a pipeline?"

With this principled framework for operator valuation established, we can now devise a strategy for constructing high-performance pipelines.

3.2 Position-Aware Shapley-Guided Pipeline Construction

In this section we present our core algorithmic contribution: a principled method for constructing pipelines by leveraging position-specific Shapley values. Unlike prior applications of Shapley values in machine learning that focus on static feature attribution [18] or data valuation [19], adapting Shapley values to sequential pipeline construction is non-trivial and requires careful formulation to capture order-dependent operator interactions. Classical Shapley values, which assume order-independent contributions, cannot capture this behavior. We address this by introducing Conditional Position-Specific Shapley values.

Definition 6 (Conditional Position-Specific Shapley). For position j with an already-selected prefix $P_{< j}^* = [o_1^*, \dots, o_{j-1}^*]$, the conditional Shapley value of operator o_i is its expected marginal contribution over all possible suffix pipelines:

$$\phi_i^{(j)}(P_{< j}^*) = \mathbb{E}_{q \sim Uniform(\mathcal{S}_{M-j})}[\Delta_i(P_{< j}^* \oplus o_i \oplus q, j)]$$
(5)

where $\Delta_i(\cdot) = v(P^*_{\leq j} \oplus o_i \oplus q) - v(P^*_{\leq j} \oplus \emptyset \oplus q)$ is the marginal contribution, \oplus denotes concatenation, and $S_{M-j} = (\mathcal{O} \cup \{\emptyset\})^{M-j}$ is the space of all possible suffixes of length M-j.

This formulation naturally extends classical Shapley values to sequential settings by conditioning on the pipeline prefix and averaging over future contexts. It evaluates each operator in the actual position where it will be placed, ensuring that the Shapley value reflects position-dependent behavior.

Algorithm 1 formalizes this position-aware construction strategy. For each position j (Line 2), we compute the conditional Shapley value for every candidate operator $o_i \in \mathcal{O}$ (Lines 4-13). The core computation involves exhaustive enumeration over all possible suffix pipelines (Line 7), evaluating the operator's marginal contribution in each context (Lines 8-10), and averaging these contributions (Line 12). The operator with the highest Shapley value is then selected for the current position (Line 14) and appended to the growing pipeline (Line 15).

3.3 The Computational Barrier

Despite its theoretical elegance, the position-aware Shapley approach faces a critical computational barrier. As formalized in Theorem 1, this method requires exponential evaluations.

Theorem 1 (Complexity of Position-Aware Shapley Construction). Algorithm 1 requires computing conditional Shapley values at M positions, each evaluating N operators across all possible suffixes, leading to a total evaluation count of:

$$T_{exact} = \sum_{j=1}^{M} N \cdot (N+1)^{M-j} \cdot 2$$

$$= N \cdot \frac{(N+1)^{M} - 1}{N} \cdot 2 \approx 2(N+1)^{M}$$
(6)

Proof. At position j, we evaluate N candidate operators. For each candidate, we must enumerate all $(N+1)^{M-j}$ possible suffixes (the +1 accounts for the null operator \emptyset). Each suffix requires 2 evaluations (with and without the candidate operator) to compute its marginal contribution. Summing across all M positions yields a geometric series that simplifies to the expression above.

To illustrate the scale of this problem, consider a typical scenario with N=25 operators and a pipeline length of M=6. Theorem 1 implies over $2\times 26^6\approx 6.1\times 10^8$ evaluations. At 60 seconds per evaluation, this would require approximately 1,170 years of computation. Even Monte Carlo sampling to approximate the Shapley values remains prohibitively expensive, requiring thousands of evaluations. This computational barrier renders the direct approach impractical, motivating our hierarchical solution.

4 HIERARCHICAL SHAPLEY SEARCH

To overcome the exponential complexity barrier, we introduce Hierarchical Shapley Search (ShapleyPipe), an approach that exploits the natural categorical structure of operator libraries to decompose the problem into a tractable, two-stage process.

Algorithm 1 Position Shapley-Guided Pipeline Construction

```
Input: Operator library \mathcal{O} = \{o_1, \dots, o_N\}, pipeline length M
Output: Pipeline P^* = [o_1^*, \dots, o_M^*]
1: Initialize P_{<1}^* \leftarrow []
    2: for j = 1 to M do
                 // Evaluate every possible candidate operator
                 for each operator o_i \in \mathcal{O} do
    4:
                       \phi_i^{(j)}(P_{< j}^*) \leftarrow 0 \\ \textit{// exhaustive suffix enumeration}
    5:
    6:
                       for each suffix q \in \mathcal{S}_{M-j} do

Evaluate v_{\text{with}} \leftarrow v(P^*_{< j} \oplus o_i \oplus q)

Evaluate v_{\text{without}} \leftarrow v(P^*_{< j} \oplus \emptyset \oplus q)
    7:
    8:
    9:
                \phi_i^{(j)}(P_{< j}^*) \leftarrow \phi_i^{(j)}(P_{< j}^*) + (v_{\text{with}} - v_{\text{without}})
\text{end for}
\phi_i^{(j)}(P_{< j}^*) \leftarrow \phi_i^{(j)}(P_{< j}^*)/|\mathcal{S}_{M-j}|
\text{end for}
  10:
  11:
  12:
14: o_{j}^{*} \leftarrow \arg\max_{o_{i} \in \mathcal{O}} \phi_{i}^{(j)}(P_{< j}^{*})
15: P_{< j+1}^{*} \leftarrow P_{< j}^{*} \oplus o_{j}^{*}
16: end for
                                                                                                                                                                                        // Append the best operator for this position
 17: return P^*
```

4.1 A Two-Stage Hierarchical Decomposition

The key insight is that data preparation operators naturally partition into a small number of functional categories (e.g., Imputation, Scaling, Feature Engineering) [20]. We leverage this structure to factorize the search space.

Proposition 1 (Search Space Factorization). When operators partition into K categories with average size |C|, where $N = K \cdot |C|$, the search space factors as:

$$\underbrace{(N+1)^M}_{Flat:\ 26^6=309 Million} \approx \underbrace{(K+1)^M}_{Category:\ 6^6=46.7 K} \times \underbrace{(|C|)^M}_{Within:\ 5^6=15.6 K}$$
(7)

If we search category structures and operator assignments sequentially rather than jointly:

Two-stage:
$$(K+1)^M + (|C|)^M = 62K \ll 309M$$

This represents a **5,000**× reduction. Based on this, ShapleyPipe decomposes pipeline construction into two sequential stages:

- Stage 1: Category Structure Search. Determine an optimal sequence of abstract operator categories, such as [Imputation, Scaling, Engineering, Selection, ...]. This is a search in a much smaller space of K items.
- Stage 2: Operator-Level Refinement. Given the optimal category sequence from Stage 1, select the best specific operator for each position from within its assigned category. This involves M independent, small-scale searches.

This decomposition, as we will show, maintains the interpretability of Shapley values while making the computation feasible.

4.2 Validating the Hierarchical Assumption: The Coherence of Operator Categories

The effectiveness of our hierarchical decomposition hinges on a critical assumption: that operators within the same category behave similarly, while operators from different categories behave distinctly. We now empirically and theoretically validate this assumption.

Empirical Evidence. We conducted a systematic clustering analysis on a tractable problem scale (N=15, M=3) across 18 diverse datasets. For each operator, we constructed a behavioral signature vector of its Shapley values across all contexts. We then computed the pairwise Pearson correlation between these signatures.

Figure 2 visualizes the resulting correlation matrix, with operators grouped by expert-defined categories. The pronounced block-diagonal structure provides compelling evidence for categorical coherence. Diagonal blocks (within-category) are dark red, indicating high positive correlation ($\rho_{\rm within}=0.310\pm0.249$). Off-diagonal blocks (between-category) are predominantly blue, indicating weak to negative correlation ($\rho_{\rm between}=-0.098\pm0.235$). Furthermore, hierarchical clustering on these signatures achieved an Adjusted Rand Index (ARI) of 0.611 with expert labels, confirming that the data-driven structure aligns with human intuition.

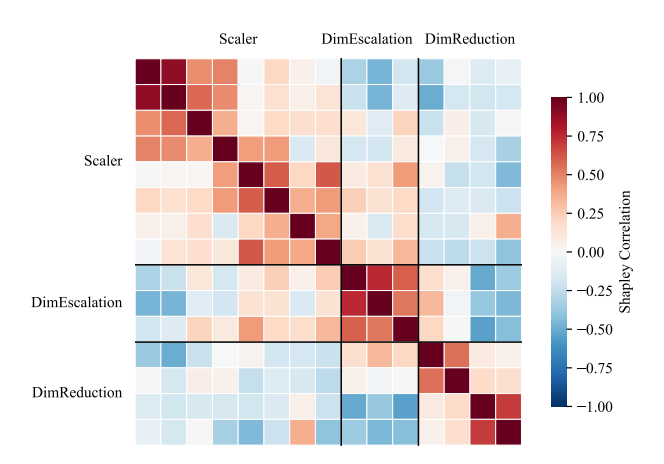


Figure 2: Correlation heatmap shows strong within-category coherence (diagonal blocks, $\rho_{\text{within}} = 0.310 \pm 0.249$) and weak between-category correlation (off-diagonal regions, $\rho_{\text{between}} = -0.098 \pm 0.235$), validating that operators partition into behaviorally distinct functional groups.

Theoretical Justification. We formalize this observation with the concept of category coherence and prove that it guarantees a bounded approximation error for our hierarchical search.

Definition 7 (Category Coherence). A partition of operators $\mathcal{O} = c_1 \cup \cdots \cup c_K$ is $(\epsilon_{intra}, \epsilon_{inter})$ -coherent if, for any position, the Shapley values of operators within any category c_i differ by at most ϵ_{intra} , and the average values between any two distinct categories c_i , c_j differ by at least ϵ_{inter} .

Theorem 2 (Factorization Approximation Quality). Suppose the operator partition is $(\epsilon_{intra}, \epsilon_{inter})$ -coherent at all positions with $\epsilon_{inter} \geq 3\epsilon_{intra}$. Let P^*_{oracle} be the true optimal pipeline and $P^*_{ShapleyPipe}$ be the pipeline constructed by ShapleyPipe. Then the performance gap is bounded by:

$$v(P_{oracle}^*) - v(P_{ShapleyPipe}^*) \le M \cdot \epsilon_{intra} + \delta_{Stage-1}$$
 (8)

where $\delta_{Stage-1}$ is the category selection error from Stage 1.

This theorem provides a formal guarantee that if categories are well-separated (a condition our empirical results support), our hierarchical decomposition introduces only a small, bounded approximation error.

4.3 Stage 1: MAB-Guided Category Structure Search

The goal of Stage 1 is to find the best sequence of categories. To do this, we must estimate the Shapley value of abstract categories like "Scaling". A key challenge is selecting a representative operator to evaluate the category's performance without exhaustively testing all its members.

To solve this, we model the selection of a representative operator within each category as a **Multi-Armed Bandit (MAB)** problem. Each operator within a category is an "arm." When we need to evaluate a category as part of a Shapley value calculation, we use an Upper Confidence Bound (UCB) policy [21, 22] to select an operator. UCB intelligently balances *exploiting* the best-performing operators seen so far with *exploring* operators whose potential is still uncertain.

$$o_{\text{next}} = \arg\max_{o \in C} \left(\bar{x}_o + \sqrt{\frac{2\ln T}{n_o}} \right) \tag{9}$$

where \bar{x}_o is the empirical mean reward for operator o, n_o is the number of times it has been selected, and T is the total number of selections.

Algorithm 2 computes category Shapley values through MAB-guided Monte Carlo sampling. For each sampled suffix sequence π (Line 2), we use UCB to select representative operators for the target category and suffix categories (Lines 4-5), evaluate the marginal contribution (Lines 7-10), and update all participating MABs with the reward signal (Lines 11-14). This provides sample-efficient learning where a single evaluation updates multiple MAB models.

4.4 Stage 2: Constrained Operator-Level Refinement

Given the optimal category sequence $C^* = [c_1^*, \dots, c_M^*]$ from Stage 1, Stage 2 selects the best concrete operator for each position using Constrained Permutation Shapley values.

Algorithm 2 Compute Category Shapley Value

```
Input: Partial pipeline P_i (positions 1 \dots j), candidate category c_i, all categories C, remaining positions m_{\text{rem}}, MAB instances
      \{MAB_k\}_{k=1}^K
Output: Shapley value \phi(c_i)
 1: \phi \leftarrow 0, n_{\text{samples}} \leftarrow 0
 2: \Pi \leftarrow \text{SamplePermutations}(C, m_{\text{rem}}, n_{\text{perm}})
                                                                                                                                  // Sample sequences with replacement
 3: for each permutation \pi \in \Pi do
         o_i \leftarrow \text{UCB-Select}(\text{MAB}_{c_i})
 4:
                                                                                                                                               // Select representative for c_i
 5:
         \pi_{\text{ops}} \leftarrow [\text{UCB-Select}(\text{MAB}_{\pi[k]}) \text{ for } k = 1 \text{ to len}(\pi)]
                                                                                                                                                // Select for other categories
 6:
         // Construct pipelines to measure marginal contribution
         P_{\text{with}} \leftarrow P_j \oplus [o_i] \oplus \pi_{\text{ops}}
 7:
         P_{\text{without}} \leftarrow P_j \oplus [\emptyset] \oplus \pi_{\text{ops}}
 8:
                                                                                                                                                   // Null operator as control
         marginal \leftarrow v(P_{\text{with}}) - \dot{v}(P_{\text{without}})
 9:
                                                                                                                                        // Evaluate marginal contribution
10:
          \phi \leftarrow \phi + \text{marginal}
11:
          UpdateMAB(MAB_{c_i}, o_i, v(P_{with}))
                                                                                                                                                  // Update for c_i's operator
          for k = 1 to len(\pi) do
12:
13:
             UpdateMAB(MAB_{\pi[k]}, \pi_{ops}[k], v(P_{with}))
                                                                                                                                               // Update for suffix operators
14:
          end for
15:
          n_{\text{samples}} \leftarrow n_{\text{samples}} + 1
16: end for
17: \phi \leftarrow \phi/n_{\text{samples}}
18: return \phi
```

Constrained Permutation Shapley. The key innovation is that we restrict permutation sampling to sequences respecting the category ordering C^* . This correctly captures operator interactions *within* the high-level structure found in Stage 1.

Algorithm 3 presents the complete procedure. Line 4 builds the final operator pipeline P^* by iterating through the positions j of the optimal category sequence C^* . For each position, it computes the Shapley value for every candidate operator o_i within the designated category c_j^* (Lines 5–18). The algorithm's efficiency stems from the SampleConstrainedPermutations function in Line 8. This function dramatically prunes the search space by only generating operator permutations π that strictly adhere to the pre-determined category ordering of the suffix, $C^*[j+1:M]$. For each candidate operator, a fixed number of these constrained permutations (n_{perm}) are sampled to estimate its Shapley value. Within the sampling loop (Lines 9–15), the marginal contribution of each candidate o_i is calculated and aggregated. Finally, the operator with the highest computed Shapley value is selected for the current position and appended to the final pipeline (Lines 19–20). The algorithm returns both the constructed pipeline P^* and a map of the computed Shapley values Φ^{op} for subsequent interpretability analysis.

Why not greedy selection? A natural question is whether we could simply select operators greedily (i.e., pick the operator maximizing immediate validation performance) to avoid Shapley computation. We evaluate this alternative in our ablation study (Section 5.5) and find that greedy selection achieves only 0.803 accuracy compared to Shapley-guided 0.835, demonstrating that context-aware evaluation across diverse suffixes is essential for optimal selection.

Theoretical Guarantees. The reliability of our Stage 1 search is supported by two key theoretical guarantees concerning our estimation process.

First, our Shapley value estimator for categories is unbiased, and its variance decreases with the number of samples.

Lemma 1 (Category Shapley Estimation). Let $\hat{\phi}(c_i)$ denote the estimated Shapley value for category c_i from Algorithm 2 with n_{perm} samples, and let $\phi_{true}(c_i)$ be the true Permutation Shapley value (assuming perfect MAB convergence). Then:

$$\mathbb{E}[\hat{\phi}(c_i)] = \phi_{true}(c_i), \quad and \quad Var[\hat{\phi}(c_i)] = \frac{\sigma^2}{n_{perm}}$$
(10)

where σ^2 is the variance of marginal contributions across permutations.

Proof. The estimator $\hat{\phi}$ is the sample mean of marginal contributions (Line 11 in original Algorithm 2). Each marginal contribution is an unbiased sample from the Permutation Shapley distribution (due to uniform permutation sampling, Line 2). The result follows from the properties of sample means.

Second, the UCB algorithm used for representative selection is guaranteed to converge to the best operators with logarithmic regret, ensuring our category evaluations are accurate and efficient.

Algorithm 3 Constrained Permutation Shapley

```
Input: Category sequence C^*, number of samples n_{\text{perm}} Output: Operator pipeline P^*, operator Shapley values \Phi^{\text{op}}
  1: P^* \leftarrow [], \Phi^{op} \leftarrow empty\_map
  2: // Build final pipeline based on the given category sequence C^*
  3: for position j = 1 to M do
  4:
           // Evaluate all candidates from the designated category
  5:
           for each operator o_i \in c_i^* do
                \phi(o_i) \leftarrow 0, n_{\text{samples}} \leftarrow 0
  6:
               // The core efficiency mechanism is constrained sampling:
  7:
  8:
               \Pi \leftarrow \text{SampleConstrainedPermutations}(C^*[j+1:M], n_{\text{perm}})
  9:
               for each permutation \pi \in \Pi do
10:
                     P_{\text{with}} \leftarrow P^* \oplus [o_i] \oplus \pi
                    P_{\text{without}} \leftarrow P^* \oplus [\emptyset] \oplus \pi
\text{marginal} \leftarrow v(P_{\text{with}}) - v(P_{\text{without}})
11:
12.
                    \phi(o_i) \leftarrow \phi(o_i) + \text{marginal}
13:
14:
                    n_{\text{samples}} \leftarrow n_{\text{samples}} + 1
15:
                end for
                \phi(o_i) \leftarrow \phi(o_i)/n_{\text{samples}}
\Phi^{\text{op}}[j, o_i] \leftarrow \phi(o_i)
16:
17.
18:
                                                                                                                                                       // Select best operator for position j
19:
           o^* \leftarrow \arg\max_{o \in c_i^*} \phi(o)
            P^* \leftarrow P^* \oplus [o^*]
20:
21: end for
22: return P^*, \Phi^{op}
```

Theorem 3 (MAB Regret Bound). Let o_k^* be the best operator (arm) in category C_k . After T selections from C_k using UCB, the expected cumulative regret is bounded by:

$$E[R_T] = \sum_{t=1}^T E[v(o_k^*) - v(o_t)] = O\left(\sum_{o \in C_k, o \neq o_k^*} \frac{\ln T}{\Delta_o}\right)$$

$$\tag{11}$$

where $\Delta_o = v(o_k^*) - v(o)$ is the performance gap of a suboptimal operator o.

This logarithmic regret ensures that UCB quickly identifies and converges to high-quality operators, making the MAB-based estimation both accurate and sample-efficient.

4.5 Complexity Analysis

Having detailed the ShapleyPipe framework, we now formally analyze its computational cost to demonstrate that it successfully overcomes the barrier identified in Section 3.3.

Theorem 4 (Hierarchical Complexity). The two-stage ShapleyPipe method, using MAB-guided search in Stage 1 and constrained search in Stage 2, requires a total number of evaluations of:

$$T_{ShapleyPipe} = \underbrace{M \times K \times n_{perm} \times 2}_{Stage\ 1:\ Category\ Shapley} + \underbrace{M \cdot |C| \cdot n'_{perm} \cdot 2}_{Stage\ 2:\ Operator\ Refinement} \tag{12}$$

where K is the number of categories ($K \ll N$), and n_{perm} , n'_{perm} are the permutation sample sizes.

Proof. Stage 1 computes Shapley values for K categories at each of the M positions using Monte Carlo sampling. Stage 2 computes constrained Shapley values for an average of |C| operators at each of the M positions. The complexity is polynomial in the problem parameters and linear in the sampling sizes, a dramatic reduction from the exponential $O((N+1)^M)$ complexity of the baseline.

For our standard settings (M=6, N=25, K=5, $n_{\rm perm}$, $n'_{\rm perm}=75$), ShapleyPipe requires approximately **9,000 evaluations**. This represents a speedup of over **34,000x** compared to the naive exhaustive baseline. This confirms that ShapleyPipe makes the Shapley-guided search for data preparation pipelines practically achievable.

Table 1: Dataset characteristics used in our experiments. Datasets are sourced from the DiffPrep benchmark collection.

Dataset	Samples	Features	Classes	Domain
abalone	4,177	8	28	Marine Biology
ada_prior	4,147	14	2	Classification
avila	20,867	10	12	Pattern Recognition
connect-4	67,557	42	3	Game Theory
eeg	14,980	14	2	Signal Processing
google	4,584	8	2	Web Analytics
house	22,784	80	2	Real Estate
jungle_chess	44,819	6	3	Game AI
micro	10,992	20	5	Microscopy
mozilla4	15,545	5	2	Software Metrics
obesity	2,111	16	7	Health
page-blocks	5,473	10	5	Document Analysis
pbcseq	1,945	18	2	Medical Sequences
pol	15,000	48	2	Political Science
run_or_walk	88,588	6	2	Activity Recognition
shuttle	58,000	9	7	Aerospace
uscensus	32,561	14	2	Demographics
wall-robot-nav	5,456	24	4	Robotics

5 Experiments

To comprehensively evaluate the effectiveness, efficiency, and interpretability of our proposed ShapleyPipe framework, we conducted a series of extensive experiments. Our evaluation is structured around four core research questions (RQs):

- RQ1(Effectiveness): How does the quality of pipelines discovered by ShapleyPipe compare to state-of-the-art methods across diverse datasets?
- RQ2(Efficiency): How do ShapleyPipe's runtime, evaluation count, and cost-performance compare to baselines?
- RQ3(Interpretability): Do the Shapley values computed by ShapleyPipe provide meaningful and actionable insights into the pipeline construction process?
- RQ4(Component Contributions): What is the contribution of each component (hierarchy, MAB, Shapley)?

5.1 Experimental Setup

Datasets. We evaluate on 18 datasets from the DiffPrep benchmark [23], a standard collection for automated data preparation research. As summarized in Table 1, these datasets span diverse domains (e.g., biology, finance, computer vision), and vary substantially in size (1,945 to 88,588 samples), dimensionality (5 to 80 features), and task complexity (2 to 28 classes). This diversity ensures a robust assessment of each method's generalization capabilities.

Operator Library. We construct a comprehensive library of 25 common preprocessing operators, organized into 5 functional categories as shown in Table 2. This library covers a wide range of transformations, including imputation, encoding, scaling, feature engineering, and selection, reflecting practical machine learning scenarios. All operators are implemented using scikit-learn with their default parameters.

Baseline Methods. We compare ShapleyPipePipe against a comprehensive suite of baselines that represent different AutoML paradigms:

- Classic Heuristics: Random Search (RS) uniformly samples pipelines until budget exhaustion. Greedy Sequential (Greedy) builds pipelines position-by-position, selecting the operator that maximizes immediate validation performance without Shapley values.
- Evolutionary Algorithms: TPOT [5] and SAGA [10], both popular and powerful genetic algorithm-based methods.
- **Reinforcement Learning:** CtxPipe [12], the current SOTA method for this task. HAI-AI [13] incorporates simulated human feedback into RL training.
- LLM-based AutoML: A suite of recent approaches that leverage Large Language Models (LLMs) to generate pipelines: CatDB [24] and AutoML-Agent(ML-Agent) [25] represent LLM-based approaches, using GPT-40 to generate pipelines based on dataset characteristics. GPT40-Z (Zero-shot) [26], and GPT40-F (Few-shot), direct pipeline generation using general-purpose LLMs.

• High-Budget Random Search (ES*): To assess the performance ceiling achievable with extensive random exploration, we include ES* results from CtxPipe [12]. ES* represents random search with an extended budget of 10,000 evaluations, provides a strong empirical upper bound that is computationally feasible. We emphasize that ES* does not represent the true optimal solution, but rather serves as a challenging baseline that demonstrates the quality achievable through high-budget random exploration.

Table 2: Operator library organized by functional category.

Category	Count	Representative Operators
Imputer Category	1	Most Frequent(0)
Imputer Number	3	Mean(1), Median(2), Most Frequent(3)
Encoding	3	Numeric Data(4), Label(5), One-Hot(6)
Scaling	8	MinMax(7), MaxAbs(8), Robust(9), Standard(10), Quantile Transform(11), Power Transform(12), Normalizer(13), K-Bins Discretizer(14)
Engineering	9	Polynomial(15), Interaction(16), PCA AUTO(17), PCA LAPARK(18), PCA ARPACK(19), Incremental PCA(20), Kernel PCA(21), Truncated SVD(22), Tree Embedding(23)
Selection	1	Variance Threshold(24)
Total	25	-

Hyperparameter Configuration. To ensure fair and meaningful comparison with CtxPipe, we adopt their experimental configuration. We construct pipelines of length M=6 from a library of N=25 operators organized into K=5 functional categories. All methods use prediction accuracy on a 80/20 train-validation split with LogisticRegression [27] as the base learner. For Shapley value estimation, we sample $n_{\rm perm}=75$ permutations in both Stage 1 and Stage 2. The MAB component uses UCB with exploration constant $c=\sqrt{2}$ and 2,000 pretrain samples for initialization. Experiments run on AMD EPYC 7543 CPUs with 128-core (16-worker parallelization).

Evaluation Metrics. We employ a multi dimensional evaluation framework. For effectiveness, we use accuracy for datasets, averaged over 7 independent runs (seeds 42, 128, 256, 512, 1,024, 2,025, 65,537). For efficiency, we measure wall-clock time (seconds) and pipeline evaluation count. Cost-performance trade-offs are quantified using evaluations per accuracy point and time per accuracy point. Stability is assessed convergence analysis (sampling size and MAB initialization).

5.2 RQ1: Evaluate Effectiveness

We evaluate ShapleyPipe's pipeline construction quality on a challenging setting where 6 operators are selected from a library of 25 candidates (M=6,N=25, plus operator \emptyset), yielding $(25+1)^6\approx 309$ million possible pipelines. The specific results are presented in Table 3.

Main Results. ShapleyPipe consistently demonstrates superior performance, achieving the highest average accuracy of 0.835 and the best average rank (2.58) across all 18 datasets, establishing a new state-of-the-art. Against CtxPipe (0.806), the leading RL-based method, ShapleyPipe delivers a 3.3% average accuracy improvement. A crucial question is not just whether a method outperforms its competitors, but how close it approaches the performance ceiling achievable through extensive exploration. While ES* cannot guarantee near-optimality, it provides a strong empirical reference point for the quality achievable with substantially more computational resources. ShapleyPipe's average accuracy (0.835) reaches 98.1% of ES*'s performance (0.851) while using only 83.5% of its evaluation budget (8,350 vs. 10,000). This comparison demonstrates that our Shapley-guided search achieves competitive results with fewer evaluations than high-budget random exploration. We also implemented Algorithm 1 (Section 3.2) at the same scale. As shown in Table 9, achieving 0.826 accuracy, lower than ShapleyPipe's 0.835, but requires 23,400 (Theorem 1) compared to ShapleyPipe's 9,000 evaluations (2.6× reduction) (Theorem 4).

Comparison with LLM-based Methods. Our results highlight the current limitations of LLM-based approaches. While specialized frameworks like CatDB (0.755) show promise, they do not match the performance of dedicated search algorithms. General-purpose LLMs, even with few-shot prompting (GPT4o-F: 0.786), struggle to generate optimal pipeline structures and fail on several datasets (indicated by N/A). This suggests that while LLMs possess broad knowledge, they currently lack the quantitative reasoning needed to navigate the complex interactions of a pipeline's search space. In contrast, ShapleyPipe's game-theoretic search provides a more effective solution.

Table 3: Performance Comparison on Search Space (M=6, N=25). Values show mean accuracy \pm standard deviation (in accuracy units) across 7 runs with different random seeds. Best performance is in **bold**. N/A indicates method failure (timeout).

Dataset	ES*	RS	TPOT	SAGA	Greedy	HAI-AI	CtxPipe	GPT4o-ZS	GPT40-FS	CatDB	ML-Agent	ShapleyPipe
abalone	0.287	0.243	0.289	0.271	0.276	0.260	0.287	0.267	0.250	0.258	0.273	0.272 (±0.5%)
ada_prior	0.857	0.844	0.823	0.846	0.840	0.801	0.818	0.839	0.831	0.835	0.838	0.843 (±0.4%)
avila	0.916	0.598	0.593	0.633	0.754	0.630	0.759	0.609	0.679	0.739	0.570	0.920 (±3.6%)
connect-4	0.792	0.671	0.658	0.702	0.794	0.775	0.763	0.713	0.657	0.759	N/A	0.794 (±0.0%)
eeg	0.861	0.658	0.594	0.683	0.737	0.556	0.740	0.623	0.834	0.529	0.556	0.801 (±4.4%)
google	0.672	0.627	0.602	0.661	0.676	0.550	0.590	0.548	0.648	0.602	N/A	0.677 (±0.6%)
house	0.955	0.938	0.941	0.952	0.928	0.928	0.818	0.904	0.928	0.906	0.926	0.924 (±1.1%)
jungle_chess	0.861	0.669	0.682	0.687	0.861	0.760	0.861	0.760	0.807	0.747	N/A	0.861 (±0.3%)
micro	0.634	0.579	0.558	0.593	0.633	0.633	0.605	0.567	0.639	0.590	0.351	0.622 (±2.0%)
mozilla4	0.940	0.922	0.890	0.927	0.940	0.870	0.940	0.867	0.931	0.820	0.856	0.935 (±0.1%)
obesity	0.927	0.841	0.942	0.874	0.877	0.768	0.868	0.851	0.816	0.724	0.676	0.917 (±0.0%)
page-blocks	0.973	0.959	0.967	0.973	0.968	0.935	0.965	0.955	0.908	0.953	0.979	0.970 (±0.8%)
pbcseq	0.866	0.730	0.715	0.725	0.766	0.733	0.805	0.704	0.694	0.644	0.756	0.757 (±1.4%)
pol	0.977	0.879	0.894	0.916	0.973	0.916	0.949	0.921	0.888	0.947	0.843	0.939 (±3.3%)
run_or_walk	0.990	0.829	0.826	0.912	0.972	0.915	0.956	0.718	0.859	0.795	0.662	0.980 (±1.0%)
shuttle	1.000	0.996	0.933	0.999	1.000	0.951	1.000	0.994	0.984	0.999	0.957	1.000 (±0.0%)
uscensus	0.854	0.840	0.828	0.852	0.826	0.807	0.845	0.841	0.851	0.851	0.749	0.848 (±0.5%)
wall-robot-nav	0.962	0.872	0.754	0.913	0.948	0.896	0.946	0.812	0.941	0.898	0.816	0.960 (±0.2%)
Average	0.851	0.761	0.749	0.784	0.821	0.760	0.806	0.750	0.786	0.755	0.721	0.835 (±1.1%)
Win Case	-	0	2	3	5	0	4	0	2	0	1	7
Rank	-	6.95	7.42	4.58	2.68	7.05	4.00	7.68	5.95	7.26	8.89	2.58

Statistical Validation. Pairwise Wilcoxon tests with Bonferroni correction ($\alpha=0.00417$) show ShapleyPipe significantly outperforms 6/9 baselines (Table 4). Against CtxPipe: mean $\Delta=+0.029, p\approx0.01$, effect size r=0.58 (larger), winning 4/18 datasets. The only non-significant comparison is Greedy (p=0.175), though ShapleyPipe wins 7/18 datasets, indicates category structure (Stage 1) provides primary value, with operator Shapley (Stage 2) offering incremental improvements.

Table 4: Pairwise statistical tests.

Baseline	W/T/L	Mean Δ	p-value	r	Sig.?
ES*	3/2/13	-0.016	0.998	-0.73	No
Random Search	16/0/2	+0.074	< 0.001	0.81	Yes*
TPOT	15/0/3	+0.086	0.001	0.77	Yes*
SAGA	14/0/4	+0.051	0.002	0.66	Yes*
Greedy	10/2/6	+0.014	0.175	0.23	No
HAI-AI	16/0/2	+0.075	< 0.001	0.85	Yes*
CtxPipe	12/2/4	+0.029	0.010	0.58	No
CatDB	15/0/3	+0.065	0.002	0.70	Yes*
ML-Agent	16/0/2	+0.115	< 0.001	0.78	Yes*

^{*} Significant at $\alpha = 0.00417$ (Bonferroni-corrected)

5.3 RO2: Computational Efficiency

We evaluate ShapleyPipe's computational cost, comparing runtime, evaluation count, and cost-performance trade-offs against baseline methods.

5.3.1 Runtime Comparison and Amortized Cost

Table 5 presents wall-clock time averaged across 18 datasets. ShapleyPipe requires 853s per dataset, with the majority of time spent on Stage 2 operator refinement. Training-based methods (CtxPipe, HAI-AI) incur one-time training overhead: CtxPipe requires 36h training + 63s validating per dataset, HAI-AI requires 3.2h + 14s validating per dataset. In contrast, ShapleyPipe operates zero-shot at 853s per dataset.

Cost Trade-offs. For a single dataset, ShapleyPipe is $152 \times$ faster than CtxPipe (853s vs. 129,663s total). However, training costs amortize across multiple datasets. CtxPipe becomes more efficient at $N \approx 164$ datasets ($\frac{129,600+63N}{N} < 853$), while HAI-AI breaks even at $N \approx 14$.

Table 5: Runtime and amortized cost comparison. Training-based methods (CtxPipe, HAI-AI) incur one-time training
overhead. Amortized cost assumes evaluation on N datasets.

Method	Per-Dataset Time (s)	Training Overhead	Amortized (N=10)
ES*	10,792	_	10,792
Random Search	194	_	194
TPOT	495	_	495
SAGA	1,495	_	1,495
Greedy	254	_	254
HAI-AI	14	3.2h (11,520s)	1,166
CtxPipe	63	36h (129,600s)	13,023
CatDB	154	_	154
AutoML-Agent	270	_	270
ShapleyPipe	853	_	853

Amortized = (Training overhead + $N \times$ Per-dataset time) / N. Table 6 reports algorithmic evaluation calls (8,350), while actual unique evaluations average \sim 5,603 (32.9% cache hit rate from deduplication). Wall-clock time (853s) reflects 16-worker (Fig. 3) parallel execution with \sim 8.73× speedup.

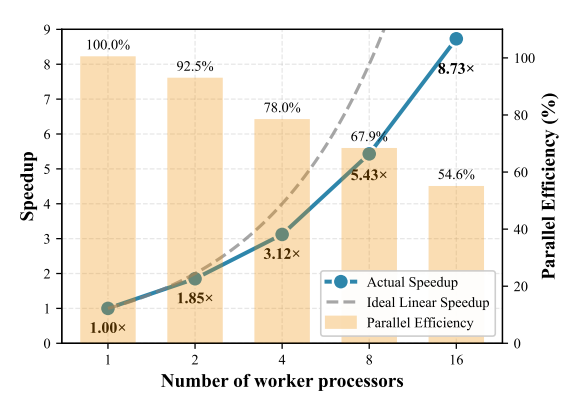


Figure 3: Parallel Scalability on ShapleyPipe

For our 18-dataset evaluation, ShapleyPipe's total cost is 15,354s ($853s \times 18$), while CtxPipe requires 130,734s (129,600s training + $63s \times 18$), ShapleyPipe is $8.5 \times$ faster overall while achieving higher accuracy (0.835 vs. 0.806). This suggests ShapleyPipe is preferable for typical research scenarios (N < 100 datasets), while training-based methods may be advantageous only in large-scale production systems where training investment can be amortized across hundreds of similar datasets.

5.3.2 Evaluation Count Analysis

The number of pipeline evaluations is a critical metric, as evaluation cost involving data transformation, model training, and cross-validation, dominates AutoML runtime. ShapleyPipe uses 8,350 total evaluations, split between Stage 1 category search (4,500) and Stage 2 operator refinement (3,850). Table 6 compares evaluation budgets across methods. Random Search uses only 100 evaluations but achieves poor accuracy (0.761). Heavy-budget methods (SAGA: 10,000, HAI-AI: 9,333) still underperform ShapleyPipe despite extensive exploration, confirming that principled search guidance matters more than evaluation volume.

5.3.3 Cost-Performance Analysis

We assess cost-benefit using two metrics: evaluations per accuracy point and time per accuracy point (lower is better).

Evaluation Efficiency. ShapleyPipe requires 10,000 evaluations per accuracy point (8,350/0.835), the most efficient among competitive methods. CtxPipe appears efficient (8 eval/acc, inference only) but including training cost (32,000 steps) yields 6,617 eval/acc. ES* demonstrates 11,751 eval/acc, confirming that Shapley-guided search is more sample-efficient than random exploration.

I	1	
Method	Evaluations	Accuracy
ES*	10,000	0.851
Random Search	100	0.761
TPOT (100 generations)	~ 1770	0.749
SAGA (15 iterations)	$\sim 10,000$	0.784
Greedy Sequential	150	0.821
HAI-AI (56,000 steps)	9,333	0.760
CtxPipe (32,000 steps)	5,333	0.806
ShapleyPipe	8,350	0.835

Table 6: Pipeline evaluations required by different methods.

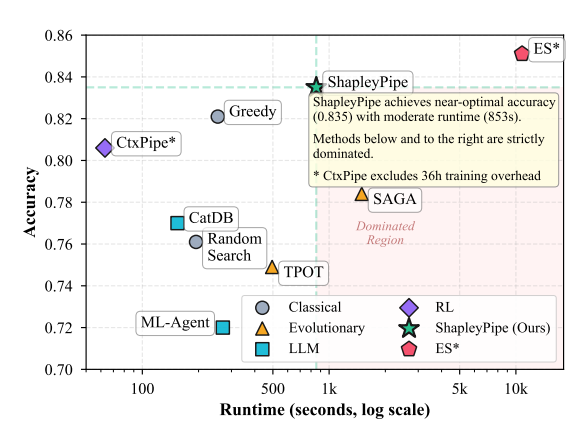


Figure 4: Accuracy-runtime Pareto frontier. ShapleyPipe (green star) achieves the highest accuracy (0.835) among methods with runtime under 1,000 seconds. Methods in the shaded region are strictly dominated. CtxPipe* excludes 36-hour training overhead.

Time Efficiency. ShapleyPipe requires 1,022 seconds per accuracy point (853s/0.835). CtxPipe inference-only appears efficient (78 sec/acc) but including 36h training yields 160,872 sec/acc. Classical methods like Random Search (131 sec/acc) and Greedy (183 sec/acc) are faster but achieve lower absolute accuracy.

Pareto Frontier. Figure 4 visualizes the accuracy-runtime trade-off. ShapleyPipe sits near the optimal frontier, achieving the best accuracy among methods with runtime under 1,000 seconds. Methods to the lower-left of ShapleyPipe are strictly dominated, both slower and less accurate. Only ES* achieves higher accuracy but requires 12.6× more time (10,792s vs. 853s), representing an unfavorable trade-off: sacrificing less than 2% accuracy gains an order-of-magnitude speedup.

5.3.4 Sampling Convergence

We systematically evaluate the impact of permutation sampling size n_{perm} on both solution quality and computational cost by varying it from 10 to 100 across all 18 benchmark datasets.

Figure 5 reveals the convergence characteristics of our Monte Carlo Shapley estimation. Accuracy improves rapidly in the early sampling regime, jumping from 0.828 at $n_{\rm perm}=10$ to 0.832 at $n_{\rm perm}=20$ (0.4% gain in 93 additional seconds). Performance continues to improve gradually, reaching a peak of 0.835 at $n_{\rm perm}=75$. Notably, further increasing to $n_{\rm perm}=100$ causes performance to decline to 0.830, representing a 0.6% drop compared to the peak. Table 7 presents the complete convergence profile. Runtime scales approximately linearly with sampling size, growing from 328s at $n_{\rm perm}=10$ to 1,152s at $n_{\rm perm}=100$ (3.5× increase), confirming $O(n_{\rm perm})$ complexity.

Convergence Stability. The narrow accuracy range of 0.831-0.835 for $n_{\text{perm}} \in [30, 75]$ demonstrates that estimates stabilize quickly, with subsequent variations of $\pm 0.2\%$ representing typical Monte Carlo sampling variance rather than systematic bias. This stability validates the robustness of our Shapley-based framework across different sampling regimes.

MAB Initialization. For MAB pretrain samples, we adopt 2,000 as default, achieving convergence with 75% variance reduction compared to minimal initialization. Details impact analysis of MAB initialization on final pipeline performance averaged across 18 datasets.

Table 7: Sampling convergence analysis averaged across 18 datasets. Performance peaks at $n_{\text{perm}} = 75$. Further increasing to $n_{\text{perm}} = 100$ degrades performance while increasing cost.

n_{perm}	Accuracy	Time (s)	Δ Acc	Δ Time
10	0.828	328	-0.7%	-62%
20	0.832	421	-0.3%	-51%
30	0.831	509	-0.4%	-40%
40	0.834	595	-0.1%	-30%
50	0.833	673	-0.2%	-21%
60	0.834	760	-0.1%	-11%
75	0.835	853	_	_
100	0.830	1,152	-0.6%	+35%

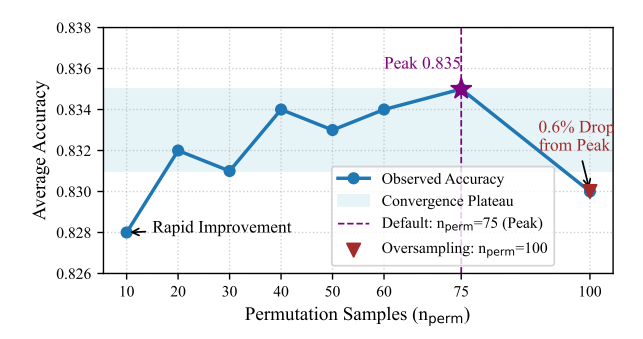


Figure 5: Accuracy convergence pattern with increasing permutation sampling size, averaged across 18 datasets. Our default $n_{\text{perm}} = 75$ (purple star) achieves peak accuracy of 0.835. Notably, further increasing to $n_{\text{perm}} = 100$ causes a 0.6% performance drop (red triangle), demonstrating that excessive sampling can degrade performance through overfitting to sampling-induced noise.

5.4 RQ3: Interpretability Validation

A key advantage of ShapleyPipe over black-box methods is interpretability: Shapley values quantify each operator's position-dependent contribution. We validate that these values provide meaningful and actionable insights through three analyses: (1) position-dependent operator behavior, (2) consistency with empirical performance, and (3) data-driven library refinement.

5.4.1 Position-Dependent Operator Valuation: A Case Study on Pbcseq

To demonstrate how Shapley values enable systematic pipeline construction, we present a detailed analysis of the Pbcseq experiment from our motivating example (Figure 1c). We exhaustively evaluated all $5^3 = 125$ pipelines from 5 operators: {ImputerMean, OneHotEncoder, RobustScaler, PolynomialFeatures, VarianceThreshold}. Table 8 shows position-specific Shapley values computed by ShapleyPipe.

Table 8: Position-Specific Shapley Values on Pbcseq

Operator	Pos 1	Pos 2	Pos 3
ImputerMean	-0.008	-0.001	0.000
OneHotEncoder	+0.002	-0.002	-0.005
RobustScaler	-0.011	0.000	+0.026
PolynomialFeatures	-0.003	+0.007	0.000
VarianceThreshold	-0.005	-0.002	-0.005

ShapleyPipe constructs the pipeline greedily by selecting the operator with maximum Shapley value at each position: OneHotEncoder (position 1, +0.002), PolynomialFeatures (position 2, +0.007), and RobustScaler (position 3, +0.026). This yields [OneHotEncoder \rightarrow PolynomialFeatures \rightarrow RobustScaler], achieving 0.743 accuracy, matching exhaustive search.

Position-Dependent Effects. RobustScaler exhibits the strongest position-dependent behavior, with Shapley values ranging from -0.011 (position 1, harmful) to +0.026 (position 3, highly beneficial), a 3.7 percentage point swing. This validates our hypothesis that operator effectiveness is fundamentally position-dependent. The suboptimal ordering [OneHotEncoder

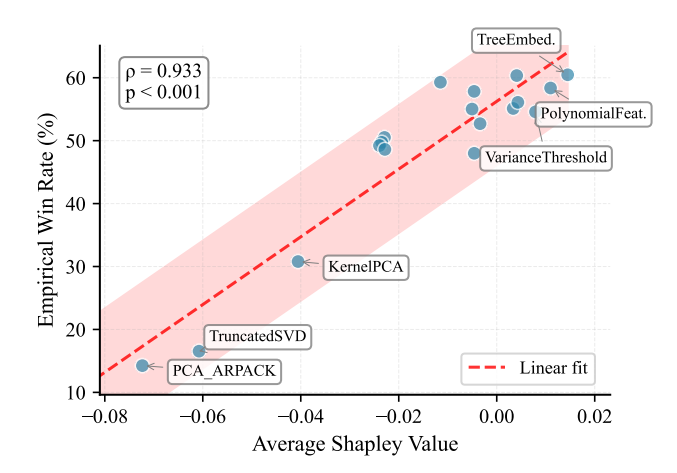


Figure 6: Correlation between average Shapley values and empirical win rates. Pearson correlation $\rho = 0.933$ (p < 0.001) demonstrates that Shapley values accurately reflect operator quality.

 \rightarrow RobustScaler \rightarrow PolynomialFeatures] achieves only 0.717 accuracy because RobustScaler contributes zero marginal value at position 2 (Shapley = 0.0), wasting a pipeline slot.

5.4.2 Consistency Between Shapley Values and Empirical Performance

To validate Shapley values reflect true operator quality, we analyze the correlation between operators' average Shapley values and their empirical performance across all datasets.

Methodology. For each operator o_i , we compute: (1) its average Shapley value $\bar{\phi}_i = \frac{1}{18M} \sum_{d,j} \phi_{i,d}^{(j)}$ across all datasets d and positions j, and (2) its empirical win rate: the percentage of pipelines containing o_i that achieve above-median accuracy. These two metrics are computed independently: Shapley values measure marginal contributions, while win rates measure absolute performance.

Figure 6 shows statistically significant positive correlation (Pearson $\rho=0.933, p<0.001$) between Shapley values and empirical win rates. Operators with high Shapley values (e.g., RandomTreesEmbedding: +0.014, PolynomialFeatures: +0.011) consistently have high win rates (60.5%, 58.4%), while operators with negative Shapley values (e.g., PCA_ARPACK: -0.072, TruncatedSVD: -0.061) have low win rates (14.2%, 16.5%). The 46.3 percentage point gap between high-quality and low-quality operators validates that Shapley values meaningfully distinguish operator contributions. This consistency confirms that our Shapley computation captures genuine operator quality rather than noise.

5.4.3 Generalization Across Datasets

This position-dependent pattern generalizes beyond Pbcseq. Analyzing 18 datasets with our full operator library, we observe systematic trends: scaling operators (e.g., StandardScaler, QuantileTransformer) achieve $2.4 \times$ higher Shapley values in early positions (1-3) versus late positions (5-6), while feature engineering operators (e.g., RandomTreesEmbedding, PolynomialFeatures) show 60% higher effectiveness when applied after preprocessing (positions \geq 3). These insights, quantified through Shapley values, stems from two design choices. Except for Hierarchical decomposition, MAB mechanism acts as implicit regularizer: UCB converges to operators with robust cross-context performance, evidenced by correlation between MAB selection frequency and rank stability (p < 0.01). Therefore, these mechanisms enable practitioners to leverage learned structure as priors while adapting specifics.

5.5 RQ4: Ablation Study

To validate our design choices, we ablated each component and measured performance degradation across 18 datasets (Table 9). The two-stage hierarchy proves essential: removing **Stage 2** (category-only) causes 12.4% degradation (0.711). while replacing it with greedy selection (maximizing immediate validation performance) achieves only 0.803 (-3.2%), demonstrating that Shapley-guided context-aware evaluation outperforms myopic selection. Removing **Stage 1 implements Position-Aware Shapley** (with n_{perm} =75 sampling) that maintains quality (0.826) but requires 2.6× more evaluations, confirming that hierarchical decomposition achieves the critical balance between efficiency and effectiveness. **Shapley-guided search** dramatically outperforms random sampling, which achieves only 0.700 (-13.5%), validating that context-aware contribution quantification is essential for non-myopic decisions. **Position-agnostic Shapley values** degrade performance by 10.0%, demonstrating that our Permutation Shapley formulation correctly captures the order-dependent

operator interactions illustrated in Figure 1(c). Finally, **the MAB mechanism** contributes 1.9% improvement by intelligently selecting high-quality category representatives, with initialization providing an additional 0.9% gain. The full ShapleyPipe framework (0.835) outperforms all ablated variants, demonstrating that each component addresses a distinct challenge and their synergy is necessary for optimal performance.

Table 9: Component contributions in our framework.

Variant	Acc	Δ vs. Full
ShapleyPipe (Full)	0.835	_
w/o Stage 1 (Algorithm 1, with n_perm=75)	0.826	-0.9%
w/o Stage 2 (Category-only)	0.711	-12.4%
w/o Stage 2 (Greedy-only)	0.803	-3.2%
w/o Shapley (Random sampling)	0.700	-13.5%
w/o Order-aware (Position-agnostic Shapley)	0.735	-9.8%
w Hierarchical stages, w/o MAB	0.816	-1.9%
w MAB, w/o Initialization	0.826	-0.9%

5.6 Discussion and Limitations

Category Coherence: $\rho_{\text{within}} = 0.310$ validates our assumption across 18 datasets, but weakens when operators differ in sensitivity (PowerTransformer vs. QuantileTransformer) or on unsuitable data (PCA on < 10 features). Practitioners should compute pilot Shapley correlations; if $\rho_{\text{within}} < 0.2$, refine categories or use flat search.

Experimental Scope: Following CtxPipe, we evaluate on M=6, LogisticRegression, tabular data (2K-90K samples). Validation on varying M, different learners (XGBoost, neural networks), and non-tabular modalities (time-series, text, images) remains future work.

Computational Trade-offs: 8,350 evaluations favor research settings (< 100 datasets); training-based methods amortize better at scale (> 200 datasets). For expensive evaluations, reduce n_{perm} to 30-40 for 60% speedup with < 1% accuracy loss.

6 Related Works

Automated Pipeline Construction. Existing AutoML methods fall into several categories with fundamental limitations. Search-based approaches (grid search, random search [6], Bayesian optimization [7,8]) struggle with exponential discrete search spaces. Evolutionary algorithms (TPOT [5], SAGA [10]) are prone to premature convergence and lack theoretical guarantees. Reinforcement learning methods (CtxPipe [12], HAI-AI [13]) represent current state-of-the-art but exhibit substantial performance gaps (Figure 1a: 24% below optimal) and operate as black boxes. LLM-based approaches [24, 25] struggle with quantitative reasoning for optimal operator selection. All existing methods treat pipeline construction as black-box optimization without quantifying individual operator contributions or handling position-dependent interactions (Figure 1c: same operators, different order \rightarrow 3.6% gap).

Shapley Values in Machine Learning. The Shapley value [28] has extensive ML applications, but *all prior work assumes order-independence*. SHAP [18] and variants [29, 30] quantify feature importance assuming features can be evaluated in any order. Data Shapley [19] and influence functions [31] focus on *which* data points to include, not *how to order* operations. Federated learning applications [32, 33] assume agent order is irrelevant. Prior AutoML work [34–36] treats components as static choices, not sequential operations where position determines effectiveness. Computational challenges motivate approximations [37], but these address estimation efficiency, not the search space factorization problem facing possible pipelines.

ShapleyPipe is the first to apply Shapley values to sequential and order-dependent pipeline construction. We introduce Position-Specific Shapley Values (Definition 6) and Permutation Shapley (Algorithm 3). ShapleyPipe combines Shapley-guided search with provable efficiency and interpretable operator valuations.

Game Theory in AutoML. Game theory has emerging applications in ML optimization, including coalition formation for ensembles [38, 39] and Nash equilibrium for architecture search [40, 41]. Unlike prior work using game theory for resource allocation [42] or coordination [43], ShapleyPipe uses cooperative games to quantify marginal contributions in sequential, position-dependent settings, enabling unified optimization and interpretability.

7 Conclusion

We introduced ShapleyPipe, a novel framework for automated data preparation pipeline construction based on hierarchical Shapley value decomposition. By reframing pipeline construction as a cooperative game to precisely quantify operator contributions. By operating at a category level before refining at the operator level, and by using a Multi-Armed Bandit mechanism for efficient estimation, our approach drastically reduces computational complexity while maintaining high fidelity. Extensive experiments on 18 diverse datasets demonstrated that not only outperforms state-of-the-art reinforcement learning and emerging LLM-based methods but also produces pipelines that are highly interpretable. Future work could explore extending this framework with transfer learning capabilities to bridge the gap between robust, dataset-specific optimization and generalizable, cross-task knowledge.

AI-Generated Content Acknowledgement

During the preparation of this work we used Claude in order to improve language. We reviewed and edited the content as needed and take full responsibility for the content of the publication.

References

- [1] Michael Stonebraker, Ihab F Ilyas, et al. Data integration: The current status and the way forward. *IEEE Data Eng. Bull.*, 41(2):3–9, 2018.
- [2] Sean Kandel, Andreas Paepcke, Joseph Hellerstein, and Jeffrey Heer. Enterprise data analysis and visualization: An interview study. *IEEE Transactions on Visualization and Computer Graphics*, 18(12):2917–2926, 2012.
- [3] Salvador García, Julián Luengo, and Francisco Herrera. Data preprocessing in data mining. Springer, 2015.
- [4] Matthias Feurer, Aaron Klein, Katharina Eggensperger, Jost Springenberg, Manuel Blum, and Frank Hutter. Efficient and robust automated machine learning. In *Advances in Neural Information Processing Systems*, pages 2962–2970, 2015.
- [5] Randal S Olson, Nathan Bartley, Ryan J Urbanowicz, and Jason H Moore. Evaluation of a tree-based pipeline optimization tool for automating data science. In *Proceedings of the genetic and evolutionary computation conference* 2016, pages 485–492, 2016.
- [6] James Bergstra and Yoshua Bengio. Random search for hyper-parameter optimization. *The journal of machine learning research*, 13(1):281–305, 2012.
- [7] Jasper Snoek, Hugo Larochelle, and Ryan P Adams. Practical bayesian optimization of machine learning algorithms. *Advances in neural information processing systems*, 25, 2012.
- [8] Chris Thornton, Frank Hutter, Holger H Hoos, and Kevin Leyton-Brown. Auto-weka: Combined selection and hyperparameter optimization of classification algorithms. In *Proceedings of the 19th ACM SIGKDD international conference on Knowledge discovery and data mining*, pages 847–855, 2013.
- [9] Bobak Shahriari, Kevin Swersky, Ziyu Wang, Ryan P Adams, and Nando De Freitas. Taking the human out of the loop: A review of bayesian optimization. *Proceedings of the IEEE*, 104(1):148–175, 2015.
- [10] Shafaq Siddiqi, Roman Kern, and Matthias Boehm. Saga: a scalable framework for optimizing data cleaning pipelines for machine learning applications. *Proceedings of the ACM on Management of Data*, 1(3):1–26, 2023.
- [11] Agoston E Eiben and James E Smith. Introduction to evolutionary computing. Springer, 2015.
- [12] Haotian Gao, Shaofeng Cai, Tien Tuan Anh Dinh, Zhiyong Huang, and Beng Chin Ooi. Ctxpipe: Context-aware data preparation pipeline construction for machine learning. *Proceedings of the ACM on Management of Data*, 2(6):1–27, 2024.
- [13] Sibei Chen, Nan Tang, Ju Fan, Xuemi Yan, Chengliang Chai, Guoliang Li, and Xiaoyong Du. Haipipe: Combining human-generated and machine-generated pipelines for data preparation. *Proceedings of the ACM on Management of Data*, 1(1):1–26, 2023.
- [14] Richard S Sutton and Andrew G Barto. Reinforcement learning: An introduction. MIT press, 2018.
- [15] Dorian Pyle. Data preparation for data mining, volume 1. Morgan Kaufmann, 1999.
- [16] Roger B Myerson. Game theory: analysis of conflict. Harvard University Press, 1991.
- [17] Eyal Winter. The shapley value. Handbook of game theory with economic applications, 3:2025–2054, 2002.

- [18] Scott M Lundberg and Su-In Lee. A unified approach to interpreting model predictions. *Advances in neural information processing systems*, 30, 2017.
- [19] Amirata Ghorbani and James Zou. Data shapley: Equitable valuation of data for machine learning. In *International conference on machine learning*, pages 2242–2251. PMLR, 2019.
- [20] Isabelle Guyon and André Elisseeff. An introduction to variable and feature selection. *Journal of Machine Learning Research*, 3:1157–1182, 2003.
- [21] Aurélien Garivier and Eric Moulines. On upper-confidence bound policies for switching bandit problems. In *International conference on algorithmic learning theory*, pages 174–188. Springer, 2011.
- [22] Tor Lattimore and Csaba Szepesvári. Bandit algorithms. Cambridge University Press, 2020.
- [23] Peng Li, Zhiyi Chen, Xu Chu, and Kexin Rong. Diffprep: Differentiable data preprocessing pipeline search for learning over tabular data. *Proceedings of the ACM on Management of Data*, 1(2):1–26, 2023.
- [24] Saeed Fathollahzadeh, Essam Mansour, and Matthias Boehm. Catdb: Data-catalog-guided, llm-based generation of data-centric ml pipelines. *Proc. VLDB Endow.*, 18(8):2639–2652, September 2025.
- [25] Patara Trirat, Wonyong Jeong, and Sung Ju Hwang. Automl-agent: A multi-agent llm framework for full-pipeline automl, 2025.
- [26] OpenAI. Gpt-4 technical report, 2024.
- [27] David Ruppert. The elements of statistical learning: data mining, inference, and prediction, 2004.
- [28] Lloyd S Shapley et al. A value for n-person games. 1953.
- [29] Scott M Lundberg, Gabriel Erion, Hugh Chen, Alex DeGrave, Jordan M Prutkin, Bala Nair, Ronit Katz, Akshay Himmelfarb, Nisha Bansal, and Su-In Lee. From local explanations to global understanding with explainable ai for trees. *Nature Machine Intelligence*, 2(1):56–67, 2020.
- [30] Avanti Shrikumar, Peyton Greenside, and Anshul Kundaje. Learning important features through propagating activation differences. In *Proceedings of the 34th International Conference on Machine Learning*, pages 3145–3153. PMLR, 2017.
- [31] Pang Wei Koh and Percy Liang. Understanding black-box predictions via influence functions. In *Proceedings of the 34th International Conference on Machine Learning*, pages 1885–1894. PMLR, 2017.
- [32] Tianhao Wang, Johannes Rausch, Ce Zhang, Ruoxi Jia, and Dawn Song. A principled approach to data valuation for federated learning. In Federated Learning: Challenges, Methods, and Future Directions, pages 153–167. Springer, 2020.
- [33] Zelei Liu, Yuanyuan Chen, Han Yu, Yang Liu, and Lizhen Cui. Gtg-shapley: Efficient and accurate participant contribution evaluation in federated learning. *ACM Transactions on Intelligent Systems and Technology*, 13(4):1–21, 2022.
- [34] Xuanyi Dong and Yi Yang. Nas-bench-201: Extending the scope of reproducible neural architecture search. In *Proceedings of the International Conference on Learning Representations*, 2020.
- [35] Frank Hutter, Holger H Hoos, and Kevin Leyton-Brown. An efficient approach for assessing hyperparameter importance. In *Proceedings of the 31st International Conference on Machine Learning*, pages 754–762. PMLR, 2014.
- [36] Yang Li, Yu Shen, Wentao Zhang, Yuanwei Chen, Huaijun Jiang, Mingchao Liu, Jiawei Jiang, Jinyang Gao, Wentao Wu, Zhi Yang, et al. Openbox: A generalized black-box optimization service. In *Proceedings of the 27th ACM SIGKDD Conference on Knowledge Discovery & Data Mining*, pages 3209–3219, 2021.
- [37] Francesco Quinzan, Vanja Doskoč, Andreas Göbel, and Tobias Friedrich. Adaptive sampling for fast constrained maximization of submodular function, 2021.
- [38] Klas Leino, Shayak Sen, Anupam Datta, Matt Fredrikson, and Linyi Li. Influence-directed explanations for deep convolutional networks. In *Proceedings of the IEEE International Test Conference*, pages 1–8. IEEE, 2018.
- [39] Yevgeniy Vorobeychik and Murat Kantarcioglu. *Adversarial Machine Learning*, volume 12 of *Synthesis Lectures on Artificial Intelligence and Machine Learning*. Morgan & Claypool Publishers, 2018.
- [40] Gabriel Bender, Pieter-Jan Kindermans, Barret Zoph, Vijay Vasudevan, and Quoc Le. Understanding and simplifying one-shot architecture search. In *Proceedings of the 35th International Conference on Machine Learning*, pages 550–559. PMLR, 2018.
- [41] Hanxiao Liu, Karen Simonyan, and Yiming Yang. Darts: Differentiable architecture search. In *Proceedings of the International Conference on Learning Representations*, 2019.

- [42] Xuebin Ren, Chia-Mu Yu, Wenjia Yu, Shusen Yang, Xinyu Yang, Julie A McCann, and Philip S Yu. Lotteryfl: Personalized and communication-efficient federated learning with lottery ticket hypothesis on non-iid datasets. *arXiv* preprint arXiv:2104.08847, 2021.
- [43] Liam Li, Kevin Jamieson, Afshin Rostamizadeh, Ekaterina Gonina, Jonathan Ben-tzur, Moritz Hardt, Benjamin Recht, and Ameet Talwalkar. A system for massively parallel hyperparameter tuning. In *Proceedings of Machine Learning and Systems*, volume 2, pages 230–239, 2020.